In-Situ Observation of Fast Surface Dynamics During the Vapor-Deposition of a Stable Organic Glass

E. Thoms,[1*] J. P. Gabriel,[1] A. Guiseppi-Elie,[2] M. D. Ediger,[3] and R. Richert[1]

[1] *School of Molecular Sciences, Arizona State University, Tempe, Arizona 85287, United States*

[2] *Department of Biomedical Engineering, College of Engineering,Texas A&M University, College Station, Texas 77843, United States*

[3] *Department of Chemistry, University of Wisconsin-Madison, Madison, Wisconsin 53706, United States*

[*] *Corresponding author: Erik Thoms (email: ethoms@asu.edu)*

TOC GRAPHICS

Dielectric measurements record the film growth during physical vapor deposition, as well as thickness and dynamics associated with the fast surface layer.

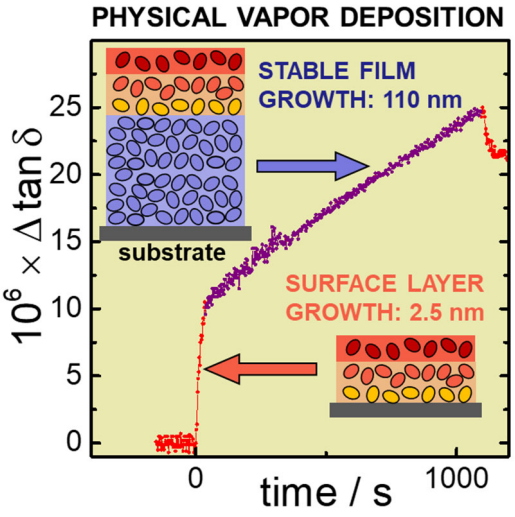

KEYWORDS: Physical vapor deposition; Glassy systems; Surface diffusion; Dielectric properties

By measuring the increments of dielectric capacitance (ΔC) and dissipation ($\Delta\tan\delta$) during physical vapor deposition of a 110 nm film of a molecular glass former, we provide direct evidence of the mobile surface layer that is made responsible for the extraordinary properties of vapor deposited glasses. Depositing at a rate of 0.1 nm s^{-1} onto a substrate at T_{dep} = 75 K = 0.82T_g, we observe a 2.5 nm thick surface layer with an average relaxation time of 0.1 s, while the glass growing underneath has a high kinetic stability. The level of $\Delta\tan\delta$ continues to decrease for thousands of seconds after terminating the deposition process, indicating a slow aging-like increase in packing density near the surface. At very low deposition temperatures, 32 and 42 K, the surface layer thicknesses and mobilities are reduced, as are the kinetic stabilities.

Glassy solids have gained importance in numerous technologies, and their performance can be further enhanced by aging, i.e., the slow approach towards equilibrium below the glass transition temperature, T_g. Using the technique of physical vapor deposition (PVD), Swallen *et al.* have demonstrated that glasses of exceedingly highly kinetic stability and density can be produced within minutes,[1,2] whereas it may require thousands or even millions of years of aging to arrive at the same desirable properties via cooling the liquid.[3] It has been rigorously established that experimental parameters that promote high kinetic stability are deposition temperatures around 0.85T_g, and deposition rates not exceeding 1 nm s^{-1}.[4] Relative to their liquid-cooled counterparts, the extraordinary properties of such glassy solids are an enhanced resistance to softening above the standard T_g (kinetic stability), an increased density, and (in some cases) anisotropy. The higher density and stability leads to a suppression

of residual molecular mobility, observable in the glass by dielectric techniques as a reduction of the loss, ε'', or dissipation $\tan\delta$.[5,6,7]

In order to obtain very dense glasses by cooling the liquid below T_g, a low temperature is required as thermodynamic driving force, but the time scales of approaching the equilibrium density become prohibitively long.[3,8] Under favorable conditions, PVD circumvents this problem by combining a low substrate temperature, T_{dep}, with a high mobility at the glass/vacuum interface. At equilibrium, both the diffusivity, D_s, and the relaxation time, τ_s, at the surface have been observed to be orders of magnitude faster than their respective bulk counterparts, D_{bulk} and τ_α.[9,10,11,12,13,14,15] Therefore, surface molecules are assumed to equilibrate effectively during PVD, unless buried by subsequent deposition in a time shorter than τ_s,[16,17] so that the resulting kinetic stability is a matter of the competition between the surface relaxation time and the deposition rate which determines the residence time of molecules at the surface.[18,19]

While much is known about surface and bulk relaxation dynamics for glasses in steady state conditions, how molecules transform from highly mobile to frozen during physical vapor deposition has not been observed *in-situ*. This study illuminates the vitrification process during vapor deposition of a polar molecular glass former by monitoring the dielectric relaxation behavior of glassy films *in situ*, i.e., during and after the deposition process. Measurements of dielectric permittivity, $\varepsilon = \varepsilon' - i\varepsilon''$, or capacitance ($C = \varepsilon' C_{geo}$) and dissipation ($\tan\delta = \varepsilon''/\varepsilon'$), monitor film growth and reveal the thickness and dynamics associated with the surface layer during vapor deposition onto high precision microlithographically fabricated interdigitated electrodes with geometric capacitance C_{geo}.[20]

We have measured the incremental capacitance, ΔC, and dissipation, $\Delta\tan\delta$, during deposition onto an interdigitated electrode (IDE) cell, ABTECH IME 1050.5-FD-Au,

using an ultraprecision capacitance bridge Andeen-Hagerling AH-2700A set to a fixed frequency of $\nu = 1$ kHz. The resolution regarding the incremental capacitance is about 50 aF, that of $\tan\delta$ is better than 10^{-6}. Details of the deposition chamber have been provided in a recent publication.[7] The sample material employed for this study is 2-methyltetrahydrofuran (MTHF), used as received fron Acros (99+%, stabilizer-free). MTHF is a polar glass forming liquid with $T_g = 91$ K and a static dielectric constant of $\varepsilon_s \approx 20$ in the highly supercooled state.[21]

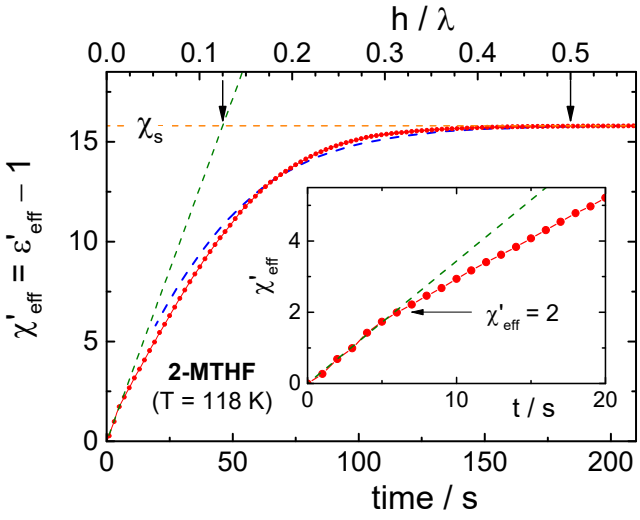

Fig. 1 Increase of $\chi'_{eff} = \Delta C/C_{geo}$ measured at $\nu = 1$ kHz during deposition (r_{dep} = 110 nm s^{-1}) of MTHF onto the IDE cell held at $T = 118$ K. Similar to the prediction limited to $h/\lambda > 0.05$ (blue dashed curve) of Igreja and Dias,[24] the χ'_{eff} data (red symbols) increases in a nonlinear fashion and saturates at the level of χ_s when $h = \lambda/2$. The linear regime (green dashed line) for which $\chi'_{eff} = \chi_s \times h/(\lambda/8)$ is limited to $h < 500$ nm, see inset.

The interpretation of dielectric data recorded during vapor deposition requires an understanding of how the capacitance changes with film thickness, h. The IDE structure on top of the borosilicate glass substrate consists of $n/2 = 50$ pairs of 100 nm thick gold-fingers with a width of $w = 10$ µm, a length of $l = 5$ mm, and a spacing of $s = 10$ µm. This pattern results in a serpentine length of $L = (s + w + l) \times (n - 1) = 49.55$ cm, a spatial periodicity $\lambda = 2(s + w) = 40$ µm, and a geometric capacitance of $C_{geo} =$

$\varepsilon_0 \times L/2 =$ 2.2 pF, where ε_0 is the permittivity of vacuum.[22] The deposition of MTHF at a constant rate of r_{dep} = 110 nm s^{-1} onto the IDE cell at T = 118 K leads to the film thickness h increasing linearly with time t, but the effective susceptibility $\chi'_{eff} = \Delta C/C_{geo}$ is not linear in h because the fringing electric field is not homogeneous. Consistent with theory,[23,24] Fig. 1 demonstrates that ΔC saturates at $h = \lambda/2$, and that the susceptibility increases with h as $\chi'_{eff} = \chi_s \times h/(\lambda/8)$ in the thin film limit, i.e., for h < 500 nm, where the field is practically homogeneous. Therefore, the following experiments are limited to $h \leq 200$ nm, so that a linear dependence of χ'_{eff} on h is secured.

The capacitance and dissipation results recorded at ν = 1 kHz while depositing up to h = 110 nm of a kinetically stable MTHF glass at r_{dep} = 0.10 nm s^{-1} onto a substrate held at T_{dep} = 75 K (= 0.82T_g) are depicted in Fig. 2. As expected, the capacitance rises approximately linearly with time, with the total ΔC = 100 fF amounting to h = 110 nm. It has been verified earlier that these deposition conditions lead to glasses of MTHF that are kinetically more stable than their liquid-cooled counterparts.[7] If this were the deposition of a film with spatially homogeneous properties, then $\Delta\tan\delta$ and ΔC should rise proportionally, i.e., both curves as scaled in Fig. 2 should coincide. Instead, for the first t = 25 s or h = 2.5 nm, the slope of $d\tan\delta/dt$ is 26 times higher and that of dC/dt is 1.3 times higher than the respective slopes for the remaining duration of the deposition process. We conclude that the first 2.5 nm layer of MTHF is in a state with higher residual mobility, and thus $\tan\delta$, with the gradual nature of the change in slope around $t \approx 25$ s suggesting a mobility gradient. Subsequent deposition for $t > 25$ s increases the thickness of the kinetically stable glass with a mobile layer of constant thickness remaining at the surface, thus exhibiting the expected uniform increase in $\tan\delta$, which persists until the deposition process is terminated. The features shown in Fig. 2 are not

specific to deposition onto the borosilicate IDE substrate, as a second 110 nm film deposited onto the first one displays the same $\Delta C(t)$ and $\Delta\tan\delta(t)$ behavior (not shown). This observation eliminates inhomogeneous or island-like growth as a relevant factor regarding the film dynamics, because the influence of the substrate is not expected to reach beyond ~ 10 nm.[25]

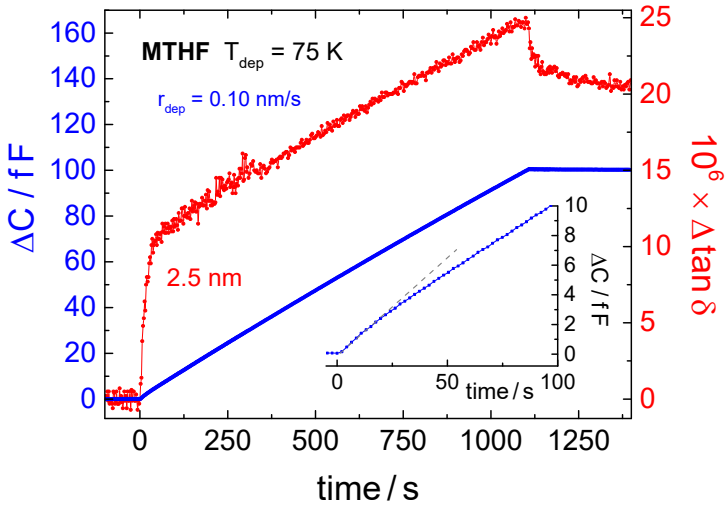

Fig. 2 Increment of capacitance, ΔC, and dissipation, $\Delta\tan\delta$, at ν = 1 kHz resulting from vapor depositing MTHF at a constant rate of r_{dep} = 0.10 nm s^{-1} onto an IDE cell held at T_{dep} = 75 K. A subtle change in the slope $d\Delta C/dt$ at $t \approx 25$ s is emphasized in the inset. Vapor deposition is initiated at t = 0 and terminated at t = 1110 s. The total ΔC increment of 100 fF corresponds to a film thickness of h = 110 nm.

In order to characterize the surface dynamics, we determine the temperature at which bulk MTHF[26] displays the same higher values of ΔC and $\Delta\tan\delta$ (relative to T = 75 K) that correspond to the behavior of the top 2.5 nm layer of PVD MTHF. It was found that at T = 94.6 K (> T_g), $\tan\delta$ is 26 times and χ' is 1.3 times higher than the respective values at T = 75 K. This suggests that (on average) the top layer is associated with dynamics reminiscent of bulk MTHF in its liquid state at 94.6 K, where the relaxation time is $\tau_\alpha \approx 0.1$ s. The value of r_{dep} implies that it takes about 5 s $\approx 50\,\tau_\alpha$ to

deposit a monolayer of MTHF, which leads to the expectation that considerable equilibration should be achieved.

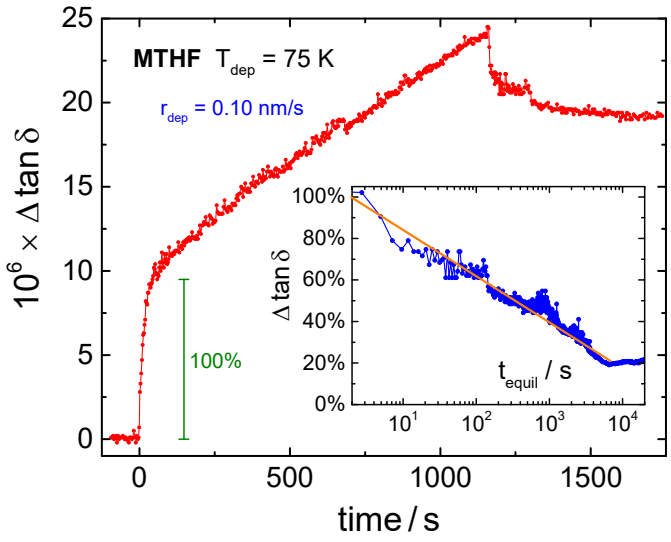

Fig. 3 Increment of the dissipation, $\Delta\tan\delta$, at ν = 1 kHz resulting from vapor depositing MTHF at a constant rate of r_{dep} = 0.10 nm s^{-1} onto an IDE cell held at T_{dep} = 75 K. Vapor deposition is initiated at t = 0 and terminated at t = 1158 s. As in Fig. 2, the total ΔC increment is 100 fF, corresponding to a film thickness of h = 110 nm. The inset shows the reduction of $\Delta\tan\delta$ after the deposition had stopped on a logarithmic time scale. Here, the change is shown as percentage of the initial fast rise, with 100 % being indicated by the vertical bar in the main frame. The levelling off near 10^4 s could be a matter of limited system stability.

The experiment using T_{dep} = 75 K (see Fig. 2) has been repeated under nominally identical conditions, and the resulting $\Delta\tan\delta$ curve is plotted in Fig. 3. Comparing Fig. 3 with Fig. 2 confirms the high reproducibility of the deposition conditions and dielectric measurements. Also, both $\Delta\tan\delta$ vs t curves appear to indicate that only about half of the liquid layer solidifies (thus reducing $\Delta\tan\delta$) after deposition has ended. However, continuing the $\Delta\tan\delta$ measurement for a long duration after the termination of PVD reveals that about 80 % of the initial fast rise (equivalent to 100 % or $\Delta\tan\delta = 9.5\times10^{-6}$, see bar in Fig. 3) disappears via a slow equilibration process, see inset of Fig. 3. A considerable (≈ 30 %) drop of $\Delta\tan\delta$ occurs within the first 25 seconds, while it continues to approach equilibrium for another ≈ 10^4 s. Note that the dielectric loss ε''

or $\tan\delta = \varepsilon''/\varepsilon'$ of a glass has been observed to correlate strongly with kinetic stability [5,7], with low loss or dissipation being indicative of higher packing density and thus more pronounced kinetic stability.

The results from repeating the experiment of Fig. 2, but at a lower T_{dep} = 32 K, are shown in Fig. 4. Similar to the T_{dep} = 75 K case of Fig. 2, the initial slope $d\tan\delta/dt$ is 24 times higher than the slope for the remaining duration of the deposition process, but a change in dC/dt is not resolved in this case. The increased slope for $\tan\delta$ persists only for the first t = 6 s or h = 0.6 nm at T_{dep} = 32 K, and the dielectric properties of this layer indicate an effective temperature of T = 89 K, where $\tau_\alpha \approx 1000$ s. From previous work it is known that the kinetic stability is marginal for T_{dep} = 32 K and r_{dep} = 0.11 nm s^{-1} compared with the T_{dep} = 75 K situation.[7] At T_{dep} = 42 K, values intermediate between 75 and 32 K are observed: the mobile layer thickness is 1.2 nm and its average dynamics correspond to those of bulk MTHF at 91 K, with $\tau_\alpha \approx 100$ s.

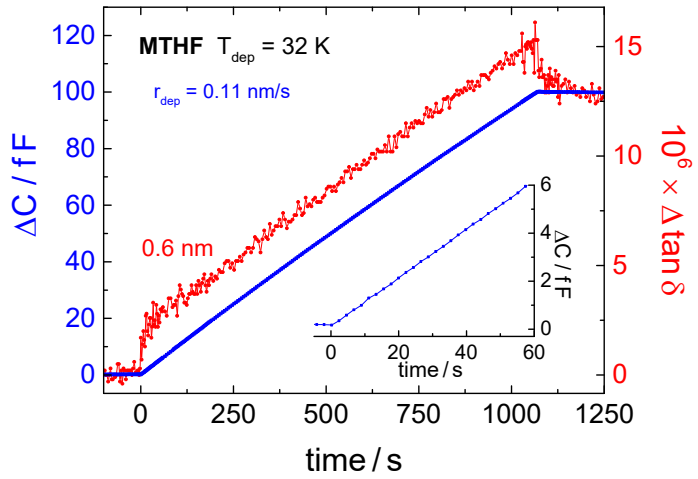

Fig. 4 Increment of capacitance, ΔC, and dissipation, $\Delta\tan\delta$, at ν = 1 kHz resulting from vapor depositing MTHF at a constant rate of r_{dep} = 0.11 nm s^{-1} onto an IDE cell held at T_{dep} = 32 K. The slope $d\Delta C/dt$ for the first 60 s of deposition is shown in the inset. Vapor deposition is initiated at t = 0 and terminated at t = 1073 s. The total ΔC increment of 100 fF corresponds to a film thickness of h = 110 nm.

What do these results tell us regarding the mobile surface layer during vapor deposition and the generation of kinetic stability of PVD films at appropriate conditions? The present technique provides quite direct detection of surface mobility, allowing the calculation of the surface relaxation time and the average thickness of the mobile region. Moreover, for the present deposition rate near 0.1 nm s^{-1} we find clear indications of the mobile layer thickness changing systematically with temperature according to 2.5, 1.2, and 0.6 nm for T_{dep} = 75, 42, and 32 K, respectively. The experiments are more indicative of a mobility gradient rather than a sample with two distinct zonal mobilities. This is consistent with previous inferences about the deposition process.[18,19]

As mentioned, the extent of mobility in the surface layer is relevant because it determines whether or not molecules have had time to relax to near the equilibrium state prior to being buried by subsequent layers of molecules. This can be quantified by the ratio of the time τ_m = 5 s required to add a monolayer (of MTHF at r_{dep} = 0.10 nm s^{-1}) to the surface relaxation time, $\tau_s(T)$. We find values of $\tau_m/\tau_s \approx 50$, 0.05, and 0.005 for T_{dep} = 75, 42, and 32 K, respectively, consistent with the higher kinetic stability for glasses deposited at 75 K relative to lower deposition temperatures.[7] The surface relaxation time $\tau_s \approx 0.1$ s found for T_{dep} = 75 K would naively indicate that surface relaxation should be complete after about 1 s. If this were true, we would not observe the slow equilibration process shown in the inset of Fig. 3 directly after stopping the vapor deposition. Given indications of a gradient in the surface mobility, we attempt to reconcile these observations as follows. While the average surface relaxation time for T_{dep} = 75 K is 0.1 s, we imagine that less mobile molecules (likely further from the interface) would require an even slower deposition rate to truly achieve equilibration during deposition. In this scenario, the entire sample is trapped in a non-equilibrium state but when the deposition is stopped, only molecules not too far from the surface

have sufficient mobility to allow further equilibration well below T_g. Consistent with this idea, the inset of Fig. 3 shows the hallmarks of a physical aging process, where further progress towards steady state is accompanied by a progressive increase of the relevant time constants. A typical signature of physical aging is that the departure from equilibrium decreases linearly with log$t$, as observed in the inset of Fig. 3. This slow component of the equilibration process suggests that very low deposition rates should give rise to a further slight enhancement of stability and packing density, an effect that has been observed for ethylcyclohexane deposited at $T_{dep} \leq 0.81T_g$.[4] It has been demonstrated that glasses with the (extrapolated) density and enthalpy of the equilibrium supercooled liquid can be obtained by PVD of ethylbenzene at $T_{dep} \geq 0.93T_g$,[27] and such glasses are not expected to display aging-like behavior after deposition.

Previous estimates of the thickness of the mobile layer are derived from steady state conditions (not during active deposition) and range from a few monolayers to 20 nm,[10,13,28,29] with no indication of a significant difference between films obtained by vapor deposition and cooling the liquid.[30] Obtaining values for the steady state thickness of the mobile layer from the present measurements has its limitations. From the decay of $\Delta\tan\delta$ after the deposition has ended, see Fig. 2 and Fig. 3, it is obvious that much of the surface mobility is lost after seconds, but subsequently $\Delta\tan\delta$ continues to drop for thousands of seconds. From the amount of $\Delta\tan\delta$ reduction observed after deposition in Fig. 3 (inset), it is difficult to derive a clear picture of the thickness and dynamics of the mobile layer that remains at steady state conditions. The curve appears to level off at 20 %, but the long time stability on $\Delta\tan\delta$ limits the interpretation of this value. That level could indicate the persistence of a mobile layer of 20%×2.5 nm = 0.5 nm thickness, but the molecules at the vacuum interface could be mobile enough to not

contribute to the dielectric loss at ν = 1 kHz. Therefore, a thin layer with dynamics much faster than 1 kHz may remain undetected by the present experiment.

In summary, this study provides an *in-situ* characterization of the fast surface layer during physical vapor deposition in terms of its average thickness and relaxation dynamics. The observations provide direct evidence for the understanding that the fast relaxation time τ_s of the surface layer facilitates equilibration at temperatures below T_g, unless a high deposition rate reduces the surface residence time to below τ_s. The picture that emerges from this study is that comparing the surface residence time τ_m with a single surface relaxation time τ_s may be too simple an explanation of how kinetic stability is established. In particular, it does not explain the slow aging-like reduction of $\Delta\tan\delta$ that suggests a further gradual approach to equilibrium after deposition had stopped. However, the observed behavior seems very reasonable for a highly stable glass prepared at a low deposition rate (but not sufficiently low to achieve the true equilibrium state). After deposition is complete, mobility near the surface will allow further slow equilibration of a small part of the sample, with regions further from the interface being slower to equilibrate. In conclusion, applying the present dielectric technique during vapor deposition for a range of deposition temperatures, deposition rates, and film thicknesses is expected to provide direct evidence for the relaxation dynamics during PVD film growth and further illuminate the origin of the extraordinary properties of PVD films. Note, however, that deposition temperatures near or above T_g will complicate the data analysis due to the structural relaxation process contributing to the permittivity.

Conflicts of interest

There are no conflicts of interest to declare.

Acknowledgements

This work was supported by the National Science Foundation under Grant No. CHE-1854930.

References

1 S. F. Swallen, K. L. Kearns, M. K. Mapes, Y. S. Kim, R. J. McMahon, M. D. Ediger, T. Wu, L. Yu and S. Satija, *Science*, 2007, **315**, 353–356.

2 L. Berthier and M. D. Ediger, *Phys. Today*, 2016, **69**, 40–46.

3 K. Dawson, L. A. Kopff, L. Zhu, R. J. McMahon, L. Yu, R. Richert and M. D. Ediger, *J. Chem. Phys.*, 2012, **136**, 094505.

4 Y. Z. Chua, M. Ahrenberg, M. Tylinski, M. D. Ediger and C. Schick, *J. Chem. Phys.*, 2015, **142**, 054506.

5 H.-B. Yu, M. Tylinski, A. Guiseppi-Elie, M. D. Ediger and R. Richert, *Phys. Rev. Lett.*, 2015, **115**, 185501.

6 C. Rodríguez-Tinoco, M. Rams-Baron, K. L. Ngai, K. Jurkiewicz, J. Rodríguez-Viejo and M. Paluch, *Phys. Chem. Chem. Phys.*, 2018, **20**, 3939–3945.

7 B. Riechers, A. Guiseppi-Elie, M. D. Ediger and R. Richert, *J. Chem. Phys.*, 2019, **150**, 214502.

8 M. D. Ediger, *J. Chem. Phys.*, 2017, **147**, 210901.

9 C. W. Brian and L. Yu, *J. Phys. Chem. A*, 2013, **117**, 13303–13309.

10 L. Yu, *Adv. Drug Deliv. Rev.*, 2016, **100**, 3–9.

11 Y. Zhang and Z. Fakhraai, *Proc. Natl. Acad. Sci.*, 2017, **114**, 4915–4919.

12 Y. Li, W. Zhang, C. Bishop, C. Huang, M. D. Ediger and L. Yu, *Soft Matter*, 2020, **16**, 5062–5070.

13 R. C. Bell, H. Wang, M. J. Iedema and J. P. Cowin, *J. Am. Chem. Soc.*, 2003, **125**, 5176–5185.

14 S. Napolitano, E. Glynos and N. B. Tito, *Rep. Prog. Phys.*, 2017, **80**, 036602.

15 N. G. Perez-de-Eulate, V. Di Lisio and D. Cangialosi, *ACS Macro Lett.*, 2017, **6**, 859–863.

16 S. Singh and J. J. de Pablo, *J. Chem. Phys.*, 2011, **134**, 194903.

17 L. Berthier, P. Charbonneau, E. Flenner and F. Zamponi, *Phys. Rev. Lett.*, 2017, **119**, 188002.

18 C. Bishop, Y. Li, M. F. Toney, L. Yu and M. D. Ediger, *J. Phys. Chem. B*, 2020, **124**, 2505–2513.

19 S. S. Dalal, D. M. Walters, I. Lyubimov, J. J. de Pablo and M. D. Ediger, *Proc. Natl. Acad. Sci.*, 2015, **112**, 4227–4232.

20 L. Yang, A. Guiseppi-Wilson and A. Guiseppi-Elie, *Biomed. Microdevices*, 2011, **13**, 279–289.

21 F. Qi, T. El Goresy, R. Böhmer, A. Döß, G. Diezemann, G. Hinze, H. Sillescu, T. Blochowicz, C. Gainaru, E. Rössler and H. Zimmermann, *J. Chem. Phys.*, 2003, **118**, 7431–7438.

22 M. C. Zaretsky, L. Mouayad and J. R. Melcher, *IEEE Trans. Electr. Insul.*, 1988, **23**, 897–917.

23 W. Olthuis, W. Streekstra and P. Bergveld, *Sens. Actuators B Chem.*, 1995, **24-25**, 252–256.

24 R. Igreja and C. J. Dias, *Sens. Actuators A*, 2004, **112**, 291–301.

25 K. Bagchi, C. Deng, C. Bishop, Y. Li, N. E. Jackson, L. Yu, M. F. Toney, J. J. de Pablo and M. D. Ediger, *ACS Appl. Mater. Interfaces*, 2020, **12**, 26717–26726.

26 A. I. Nielsen, T. Christensen, B. Jakobsen, K. Niss, N. B. Olsen, R. Richert and J. C. Dyre, *J. Chem. Phys.*, 2009, **130**, 154508.

27 M. S. Beasley, C. Bishop, B. J. Kasting and M. D. Ediger, *J. Phys. Chem. Lett.*, 2019, **10**, 4069–4075.

28 C. W. Brian, L. Zhu and L. Yu, *J. Chem. Phys.*, 2014, **140**, 054509.

29 J. D. Stevenson and P. G. Wolynes, *J. Chem. Phys.*, 2008, **129**, 234514.

30 S. Samanta, G. Huang, G. Gao, Y. Zhang, A. Zhang, S. Wolf, C. N. Woods, Y. Jin, P. J. Walsh and Z. Fakhraai, *J. Phys. Chem. B*, 2019, **123**, 4108–4117.